Engineering Geology 243 (2018) 128–144

Contents lists available at ScienceDirect

Engineering Geology

journal homepage: www.elsevier.com/locate/enggeo

Analyzing successive landslide dam formation by different triggering mechanisms: The case of the Tangjiawan landslide, Sichuan, China

Xuanmei Fan[a], Weiwei Zhan[a,b,*], Xiujun Dong[a,**], Cees van Westen[c], Qiang Xu[a], Lanxin Dai[a], Qin Yang[a], Runqiu Huang[a], Hans-Balder Havenith[d]

[a] The State Key Laboratory of Geohazard Prevention and Geoenvironment Protection (Chengdu University of Technology), Chengdu, Sichuan, China
[b] Glenn Department of Civil Engineering, Clemson University, Clemson, SC 29634, USA
[c] Faculty of Geo-Information Science and Earth Observation (ITC), University of Twente, The Netherlands
[d] Géorisques et Environnement, Université de Liège, Belgium

ARTICLE INFO

Keywords:
Landslide dams
Wenchuan earthquake
Evolution
Hazard assessment
Emergency response

ABSTRACT

The catastrophic Tangjiawan landslide, triggered by the 2008 Wenchuan earthquake, blocked the Duba River, impounding one of the most dangerous coseismic barrier lakes in Beichuan, China. The lake was drained by an artificial spillway within one month after the earthquake to minimize the potential dam-breach flooding risk. However, on September 5, 2016, this landslide was reactivated and dammed the river again, creating a 20-m high dam at the same location and resulting in the formation of a barrier lake with a volume of 0.6 million m^3. The day after the event we carried out a field investigation of the landslide and obtained a high-resolution image and DEM using UAV. The satellite images from 2005, 2008, 2010 and 2015 were also collected to analyze the evolution of the landslide. Together with multi-temporal DEMs, the geometry and volumes of the displaced mass and the landslide dams and barrier lakes were calculated using image interpretation and 3D spatial analysis with GIS. This landslide is of great scientific interest, as it presents a good example of multiple reactivation of a pre-historical giant landslide under different triggering conditions: a reactivation of an older landslide during the Wenchuan earthquake, and a second reactivation during a rainfall event several years later. Meanwhile from the hazard assessment and prevention perspective, it is also representative as it dammed the river twice in 2008 and 2016, posing threats to both upstream and downstream areas. We infer that the successive landslides in this region could be caused by the strong tectonic activities: including earthquakes and high average uplifting rate. The results of landslide volume analysis using multi-temporal DEMs, contribute to the landslide mechanism analysis, and suggest that the landslide volume estimation is effected by the landslide type, landslide rupture surface location, and resolution of DEM. We also compare the performance of different empirical models of landslide stability and dam-breach flood parameters and discuss their application during the quick assessment of the potential hazard of the landslide dams. Generally, the successive landslide dams at the Tangjiawan site are caused by the successive landslide reactivations on an anti-dip slope controlled by strong tectonic activity and river erosion, involve with a mass of loose materials of previous landslide deposition, and possess high flood risk to the downstream area. The experience gained in this work can be used to assist the hazard assessment and the planning of the emergency measures for similar landslide dams in the future.

1. Introduction

Landslide dams are common worldwide, especially in tectonically active mountain regions (Costa and Schuster, 1988; Korup, 2004; Evans et al., 2011). Many outburst floods and debris flows caused by the catastrophic release of water from landslide-impounded lakes have been documented (i.e. Mason, 1929; Cenderelli, 2000; Dai et al., 2005). After a landslide dam is formed, the foremost step is to assess its stability as well as the potential hazard and risk. Korup and Tweed (2007) concluded that the stability of landslide dams is a function of their geometry; internal structure; material properties and grain size distribution; volume and rate of water and sediment inflow; and seepage process. Landslide dams might be caused by different triggering mechanisms, although earthquakes are the most frequent trigger. Landslide dams may also be formed sequentially in the same location. For example, the Yigong landslide in southeast Tibet, China dammed

* Correspondence to: W. Zhan, Glenn Department of Civil Engineering, Clemson University, Clemson, SC 29634, USA.
** Correspondence to: X. Dong, No.1 Erxianqiao Dongsanlu, Chengdu University of Technology, Chengdu 610059, Sichuan, China.
E-mail addresses: wzhan@g.clemson.edu (W. Zhan), dongxj_sklgp@163.com (X. Dong).

https://doi.org/10.1016/j.enggeo.2018.06.016
Received 7 February 2018; Received in revised form 7 June 2018; Accepted 23 June 2018
Available online 30 June 2018

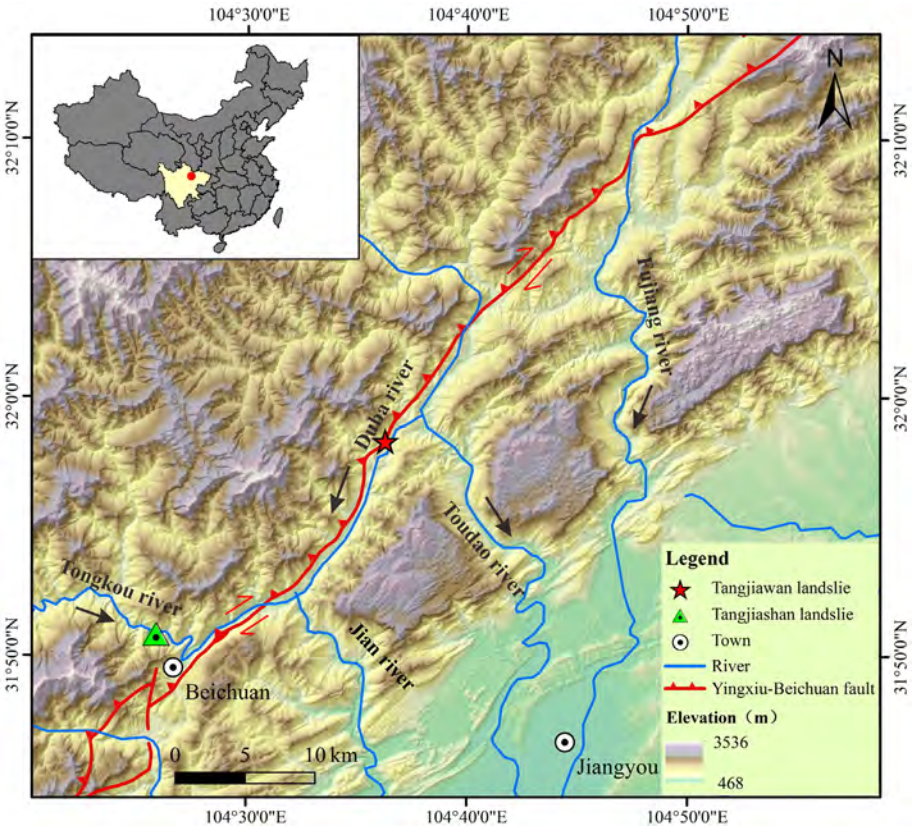

Fig. 1. Location of the Tangjiawan landslide in Beichuan, Sichuan Province.

the Zhamu Creek twice in July 1900 with a volume of 0.5 km^3 and on April 9, 2000 with a volume of 0.3 km^3 (Shang et al., 2003). Repeating damming could happen in a debris flow related environment with a sediment source in the upper catchment, which may deliver enough volumes of materials from time to time to dam the major river (Chen et al., 2015). It could also happen when a major landslide undergoes various reactivation phases over time by different triggers that deliver enough materials to block the river (Adams, 1981; Stefanelli et al., 2015). Another typical example of successive landslides occurred on the Mount Tsao-Ling, central Taiwan, where four catastrophic landslides occurred on the same slope and dammed the same river four times between 1941 and 1999. Among them two were triggered by earthquake and the other two were induced by heavy rain (Chen et al., 2006).

The M_w 7.9 Wenchuan earthquake hit China's Sichuan Province on 12 May 2008, triggering > 60,000 landslides (Görüm et al., 2011) and instantaneously forming several hundreds of landslide dams (Fan et al., 2012a). In order to reduce the potential for dam-break floods, the Chinese army created artificial spillways in 32 of the dams using explosives and heavy machinery. Xu et al. (2009) qualified the hazard of these 32 dams by considering dam height, dam composition and maximum capacity of the landslide-dammed lakes. The Tangjiawan landslide was one of the 32 most dangerous dams, which blocked the Duba River in the upstream of Chenjiaba, Beichuan, forming a lake with 1.5 million m^3 water (Shi et al., 2015). The dam was breached artificially by a spillway about one month after it was formed to control the potential dam breach flood. On September 5, 2016, the landslide was partially reactivated and dammed the river again at the same location resulting in formation of a barrier lake of a volume of about 0.6 million m^3.

The successive landslide damming events suggest the Tangjiawan site is susceptible to landslide dam hazard and might encounter landslide dam hazard in the future, providing a scarce case for both emergency measure and long-term measure for landslide dam hazard. In the view of long-term measure of landslide dam hazard, the evolution process and failure mechanism of landslides are critical, since these critical information will guide preventive measures for a potential landslide dam before its formation, such as enforcing riverbank slopes (Peng et al., 2014). For the emergency measure of landslide dam hazard, a large number of empirical or semi-empirical methods has been developed regarding risk assessment (Xu et al., 2009; Cui et al., 2009; Yang et al., 2013; Peng et al., 2014), landslide dam stability evaluation (Ermini and Casagli, 2003b; Dong et al., 2009, 2011a, 2011b; Stefanelli et al., 2016), dam breach flood hazard assessment (Costa, 1985; Evans, 1986; Costa and Schuster, 1988; Walder and O'Connor, 1997; Clague and Evans, 2000; Li, 2006; Peng and Zhang, 2012), and emergency response (Peng et al., 2014). However, significant deviation of different empirical equations exists and may result from the site-specific characteristics of the original study. The Tangjiawan landslide dammed the river twice, in 2008 and 2016, with different barrier lake volume and water level before manual breach, providing a good chance to evaluate the performance of different landslide dam hazard assessment models.

In this study, we first analyzed the evolution, the geomorphic features and the possible causal factors of 2008 coseimic landslide and 2016 reactivation landslide on the Tangjiawan slope. We then discussed the method of volume calculation using multi-temporal DEMs, and its limitation and uncertainties. Based on above analysis, we assessed the stability and hazard of the landslide dams. The potential dam-break flood parameters were estimated by empirical models and the hydraulic calculation standard that is widely used in China. The experience gained in the emergency mitigation of landslide dams was summarized and discussed.

2. Study area

The landslide is located in the Duba River valley, 6.5 km upstream

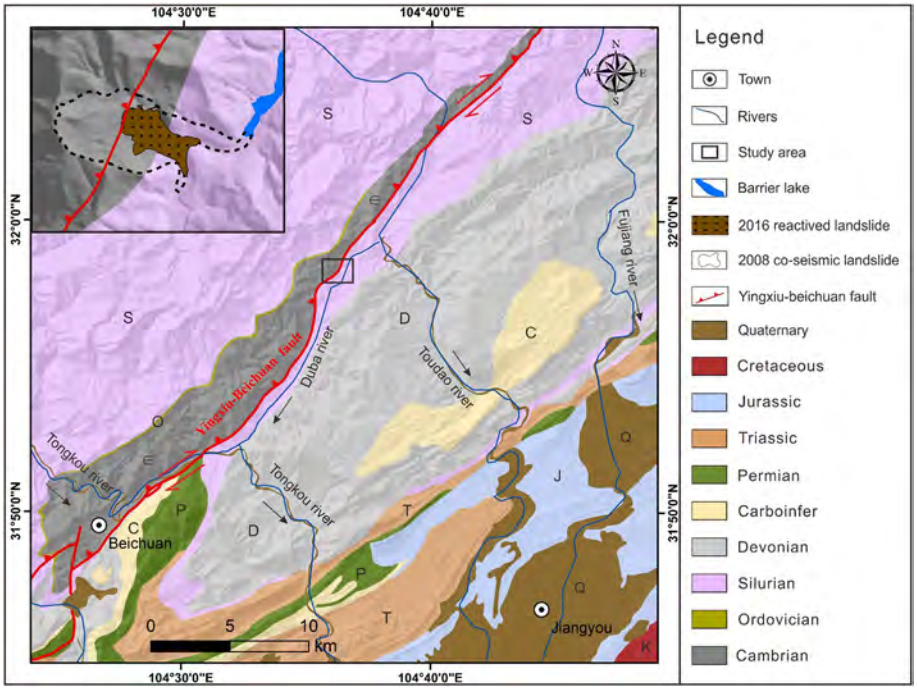

Fig. 2. Regional geologic map of the Tangjiawan landslide.

of the Chengjiaba, Beichuan (31° 58′ 23.18″N, 104° 36′ 21.33″E, Fig. 1). The Duba River is a tributary of Jian River and has a catchment area of 306 km^2. The average annual discharge is 6.2 m^3/s. According to the data from a nearby hydrologic station during the years 1970–2007, the region had a yearly average precipitation of 1399.1 mm with a maximum yearly value of 2340 mm. The maximum daily and hourly rainfall intensities are 101 mm and 32 mm, respectively. Most of the precipitation concentrates in the monsoon from June to September, accounting for about 75% of the annual precipitation.

The elevation in the area where the landslide dam and barrier lake have formed varies from 730 to 1360 m. The slope in the northern side of the river where the landslide occurred is about 35–45° on average, while slopes are more gentle in the southern side (20–25°). The study area is mainly composed of gray and black carbonaceous and siliceous shale of the Sinian epoch (end of the Neoproterozoic) covered by colluvial deposits (Fig. 2). The strata dip at 30° towards NE30° (the upstream direction of the river). The area is tectonically active, characterized by an anticlinal fold in the N-E directions and the main active fault of the Wenchuan earthquake, the Yingxiu-Beichuan fault, which had a co-seismic vertical displacement of around 5 m near Beichuan (Shen et al., 2009). The 2008 coseismic landslide initiation area is located 0.8 km from the fault surface rupture on the hanging wall, while the 2016 reactivation landslide is located near the fault surface rupture on the foot wall (Fig. 1). There are several large coseismic landslides that dammed large lakes in the nearby areas, including the largest lake dammed by the Tangjiashan landslide.

3. Evolution and failure mechanism of the Tangjiawan landslide

In order to track the activity history of this successive landslide, we collected imagery of the landslide from different sources and different years (Fig. 3). We also constructed DEMs using the pre- and post-earthquake topographic maps of 2005 (1:30000) and 2011 (1:10000), respectively. A fixed wing UAV and integrated processing software (Feima F1000 Aerial Imaging system) was used to carry out the emergency survey in September 2016. The UAV generated imagery with a spatial resolution of 7 cm and produced a very detailed Digital Surface Model (Fig. 4). Fig. 3a–d show a number of the images collected: a Google Earth image from April 2005, SPOT image from October 2008, QuickBird image from Jan, 2010 and an aerial photo from Jul 15, 2016, respectively.

3.1. Pre-historical landslide

From the image shown in Fig. 3a, which is from 2005, it is possible to observe a number of geomorphological indicators, such as the presence of linear structures, that might be indicative of a back scarp, specific micro-morphology in the middle section, and accumulation levels that might be indicative of the presence of a landslide prior to the 2008 earthquake. It could also be possible that there were two individual landslides next to each other (see Fig. 5). It is clear, however, that this landslide had dammed the Duba River, as evidence by specific accumulation levels. Based on above geomorphic features, we interpreted the boundary of an old landslide as shown in Figs. 3a and 5. We have not been able to confirm the age of the landslide with dating methods thus far.

3.2. Co-seismic landslide in 2008

The Tangjiawan landslide is triggered by the 2008 Wenchuan earthquake, claiming the lives of 150 farmers and damming the Duba River (Dai et al., 2011). The landslide was roughly estimated as 2.6 million m^3 according to the field mapping conducted by Dai et al. (2011). Based on the interpretation results of pre-earthquake and post-earthquake remote sensing images and the filed investigation, the boundary of 2008 coseismic landslide is clearly measured (Fig. 6) and a geomorphologic map of the successive landslide is completed (see Fig. 7). A profile along the main sliding direction of the coseismic failure was made based on the pre- and post- earthquake DEMs, indicating topographic changes induced by the landslide and also suggesting the evidence of the landslide mechanism (Fig. 8a).

According to Figs. 3b, 6 and 7, the 2008 coseismic landslide has a similar size as the pre-historical landslide, with the head scarp bounded by the ridge on the west, watershed on the south, and gully on the north. Fig. 6b is a photo of the landslide taken shortly after the Wenchuan earthquake in June 2008, when the dam had already been

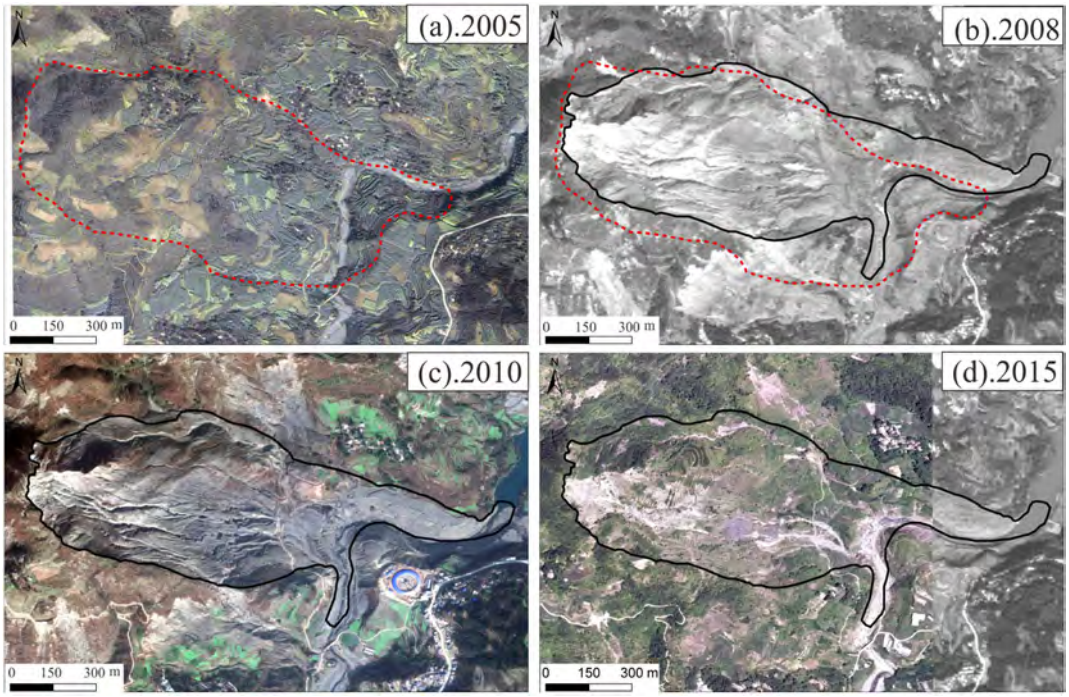

Fig. 3. Multi-temporal imagery of the Tangjiawan landside from different sources: (a) Google Earth image taken on April 13, 2005; (b) SPOT 5 image taken on October 13, 2008; (c) QuickBird image taken on Jan 13, 2010; and (d) aerial photo taken on November 17, 2015. Red dash line indicates the possible pre-historical landslide boundary mapped based on the Google Earth imagery in Fig. 4. Black line indicates the 2008 coseismic landslide boundary. (For interpretation of the references to colour in this figure legend, the reader is referred to the web version of this article.)

breached artificially. The geomorphology of the coseismic landslide can be separated to two parts by the existence of a notable cliff on the lower hillslope (Fig. 6). The slope analysis based on the high-resolution DEM obtained by UAV survey in 2016 further verify that the lower cliff exists at the Tangjiawan site and the nearby upstream pre-historical landslide site (see Fig. 9). According to Fig. 8a, it shows most of the material that depleted from the upper part of the slope deposited still in the upper part of the slope, forming a scarp of 40-60° and a concave-upward profile.

Comparing Fig. 3b (from 2010) and Fig. 3c (from 2015), it is clear that the landslide became re-vegetated in the period 2010–2015, and that the activity was reduced to several gullies on the landslide surface and the erosion of the toe of the landslide by the Duba River. According Fig. 3d, obvious rock falls can be saw on both the NE and SW boundaries of the 2016 reactivation landslide in 2015.

With regard to the failure mechanism of the 2008 coseismic landslide, we consider it as a reactivation of an old landslide according to the aforementioned geomorphic evidences. In addition, several other evidences also support this conclusion. According to a local report, geologists who did a field survey of this landslide shortly after the earthquake found ancient wood in the coseismic landslide deposit, which had been buried for a long time since the old landslide occurred. Unfortunately, no C-14 dating was carried out as the wood fragements cannot be retrieved after the 2016 reactivation. During our field investigation after the new reactivation in September 2016 (Fig. 10), we found a strongly disturbed and ruptured zone at the right (downstream)

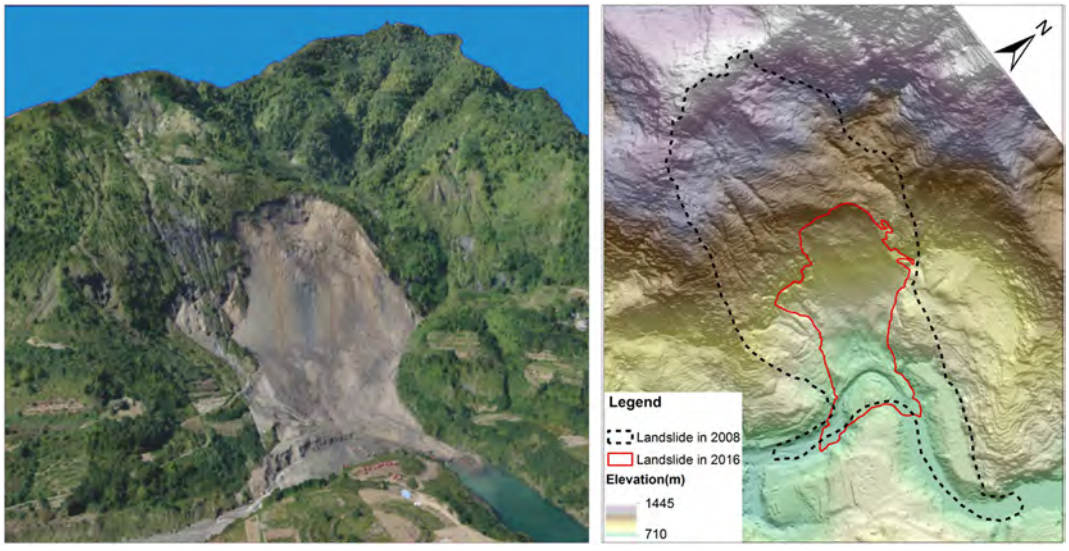

Fig. 4. Image (a) and DSM (b) of the reactivated landslide obtained by using UAV on September 6, 2016.

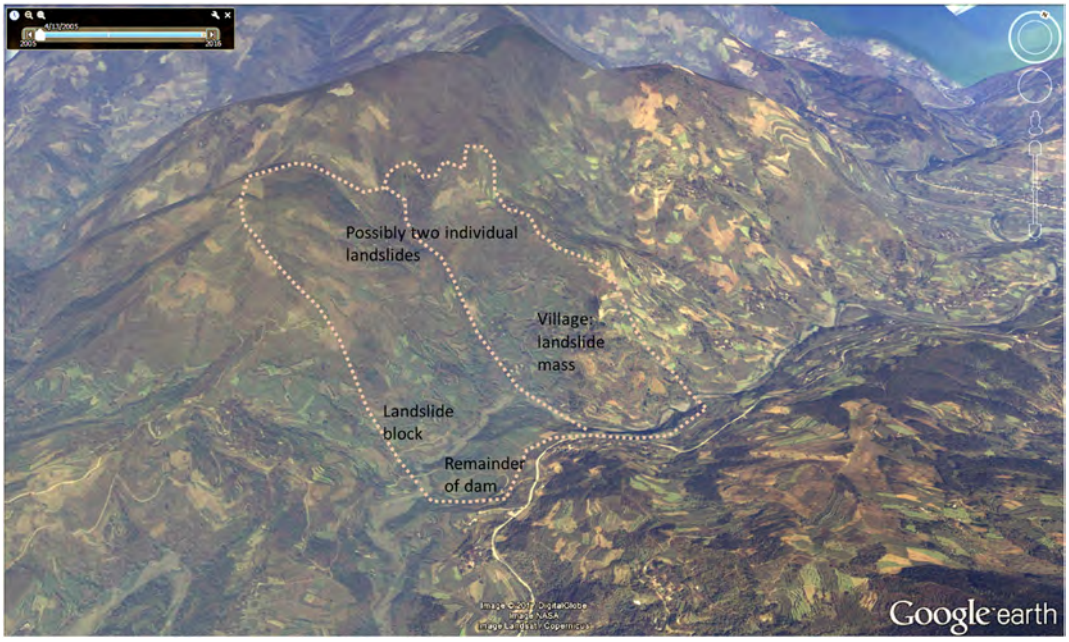

Fig. 5. Geomorphology of two pre-historical landslides at the Tangjiawan site (Google Earth image taken on April 13, 2005).

boundary of the landslide, as indicated in Fig. 11. Fig. 12 presents a closer look at this rupture zone. The material inside this zone is mainly crushed rock and plastic clays. To our best knowledge, we think this reveals the sliding surfaces of the historical movements. Dai et al. (2011) analyzed the mechanism of several large-scale landslides triggered by the Wenchuan earthquake including the Tangjiawan landslide, based on the detailed field investigation. They found the minor scarp on the landslide is coincident with the surface ruptures as observed at other measured sites, suggesting that the Yingxiu-Beichuan fault actually passed through the source area of the Tangjiawan coseismic landslide. This observation is different from the fault surface rupture mapped by Li et al. (2008) at the regional scale, which shows the fault is located at the toe of the landslide. We also observed the minor scarp in the source area of the landslide. Therefore, combined with the evidence that co-seismic relative displacement between the hanging and foot walls of Beichuan-Yingxiu fault near Beichuan was 5.1 m (Shen et al., 2009), it is more convincing that the 2008 landslide is caused by both strong ground vibration and fault oblique-thrusting force.

3.3. Reactivation landslide in 2016

On September 5, 2016, the upstream part of the lower cliff of the coseismic landslide was reactivated and dammed the river again at the same location resulting in the formation of a barrier lake (Fig. 10). The image and DSM obtained by UAV shown in Fig. 4 have a spatial resolution of 0.2 m, based on which a detailed geomorphic map of the reactivated landslide in 2016 was made as shown in Fig. 11. From Figs. 8b and 11, we could see that the new failure was developed mainly from the middle part of the coseismic landslide deposits, and the elevation of upper depletion zone ranges from 910–1010 m. It relieved the original steep scarp and formed a head scarp of about 40° on average and 100 m high (see Figs.8b and 9). The displaced material with volume about 0.323 million m^3 move downward quickly along the original middle cliff of about 60°–70° on average and hit the lower terrace consisting of the 2008 coseismic landslide deposits (see Table 1 and Fig.8b). Considering the effect of the steep (accelerated) terrain and the huge mass of initiated material, the landslide mass can generate a large amount of energy, which may cause the failure of the lower deposits. Through the detailed volume analysis based on pre-sliding and after sliding DEM, the precise geometry of the lower failure can be measured. The second failure on the lower part of 2016 landslide involved a mass of about 0.231 million m^3 and of 17.5 m deep on average, and form a head scarp of about 15.0 m high and 28°on average (see Table 1 and Fig.8b). The landslide dam is about 118 m long, 270 m wide, and its maximum height is about 20 m (see Table 2). Using the resampled 2011 DEM and 2016 DEM with spatial resolution of 1 m, the landslide dam volume was calculated to be 0.65 million^3. According to Figs. 7 and 8, it can be concluded that the dam materials are mainly from the lower failure. Highly fragmented black carbonaceous shale bedrock was exposed in the scarp. Some megaclast deposits were observed at the lower part of the slope and also at the dam site (Fig.10). Samples were obtained from the dam deposits, and the grain-size distribution was analyzed (Fig.13). Fig.13 shows that over 60% of the sample has grain sizes < 10 mm and more than 15% sample has grain sizes > 100 mm. Outcrops in the walls of the spillways but in the landslide dam body showed that the dam is mainly composed of fine materials with a small amount of large blocks and boulders.

Regarding the reactivation mechanism of 2016 landslide, the endogenic and exogenic geological processes both played an important role. The long-term tectonic activities and especially the Wenchuan earthquake caused the slope being fractured. The coseismic landslide material deposited on the steep slope is prone to fail under the external triggers, such as earthquakes and rainfalls. The landslide located at the convex bank of the river, therefore the river erosion of the toe of the landslide might reduce the stability of the landslide gradually with time. There was no intensive rain storm on the day when the landslide occurred, but there were some small antecedent rainfalls during the week before the landsliding event. According to the record from Sichuan Earthquake Administration, there were two earthquakes with magnitude 4.3 and 4.6 that occurred in Anxian on May 29, 2016 (95 km from the landslide site) and in Beichuan on June 27, 2016 (23 km from the landslide site), respectively. As described by the local farmers, small falls and slumps already started about 20 days before the big event occurred, implying that the landslide was reactivated gradually due to the combination of above effects rather than a sudden strong external force.

Considering the landslide mechanism, it is clear that this landslide-hotspot is strike by the three times landslide activities with different triggers and mechanisms. Considering the similar morphology, location and size (see Fig. 5), the prior-2008 landslide is speculated to be caused

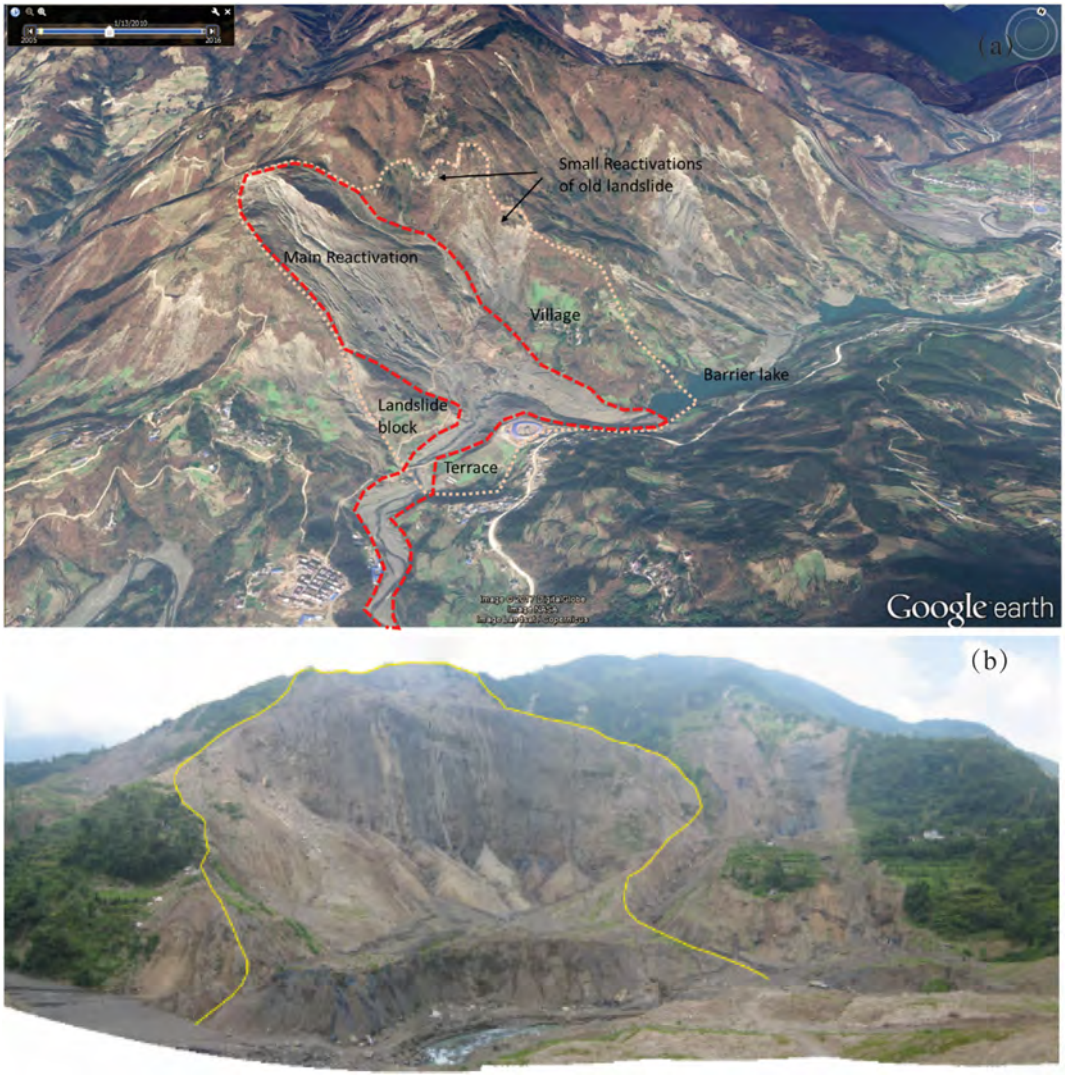

Fig. 6. Tangjiawan coseismic landslide in 2008: (A) Geomorphology of the 2008 coseismic landslide at the Tangjiawan site; (B) Photo of the Tangjiawan landslide (in front view) taken in June 2008 after the Wenchuan earthquake.

by another historic earthquake.

For the mechanism of 2016 landslide, it is much obscure as the potentials triggers (small earthquakes or rainfall) are at least one week earlier. The post-earthquake tectonic uplifting may also play a role in the 2016 reactivation. Dong et al. (2011) had reported that the uplift of the hang wall of Yingxiu-Beichuan fault was with an amplitude of 10–53 mm and a yearly rate of 5–27 mm/a near Beichuan in the period between 2008 and 2010 (tens of times of pre-earthquake rate), which is likely responsible for stress stage and rock strength variance in the slope. Besides, steep slope angles, rugged topography, river deepening and erosion at the toe of the slope are also responsible for the formation of this landslide.

4. Landslide volume analysis

Landslide volume analysis is critical for a more accurate understanding of the landslide process, and can support landslide hazard assessment and risk mitigation design. Traditionally, failure volumes are estimated through measuring landslide dimensions (length, width, and depth) on the ground, using assumptions about the shape of the landslide relative to landslide type. Such ground-based methods are time-consuming, error prone, and, sometimes not possible due to terrain inaccessibility. A more sufficient method used for calculating the landslide volume is change-detection techniques based on pre- and post- failure topographic maps that can be obtained through various ways, including the photogrammetric techniques (Martha et al., 2010). In this section, multi-temporal Digital Elevation Models have been applied for measuring the characteristics of the recent two landslide events, namely 2008 coseismic landslide and 2016 recreation landslide. The 2005 DEM with 25 m resolution is derived from the topographic map which represents the digital terrain before 2008 Wenchuan earthquake. The 2011 DEM with 5 m resolution is constructed based on a topographic map completed by a local geohazard mitigation institution in 2011. The 2016 DEM with 1 m spatial resolution is achieved through the UAV mapping on Sept 7, 2016, the next day after the slope failure.

4.1. Landslide volume estimation based on multi-temporal DEMs

The volume estimation of 2008 coseismic landslide and 2016 recreation landslide is completed on the platform of ArcGIS, and the main procedures include: use the exact function to obtain the pre-sliding and after-sliding DEMs within the landslide boundary; use the cutfill function and two extracted DEMs to calculate the landslide-caused volume variance, which in effect is calculating volumes of surface materials that have been modified by the depletion or addition of surface material

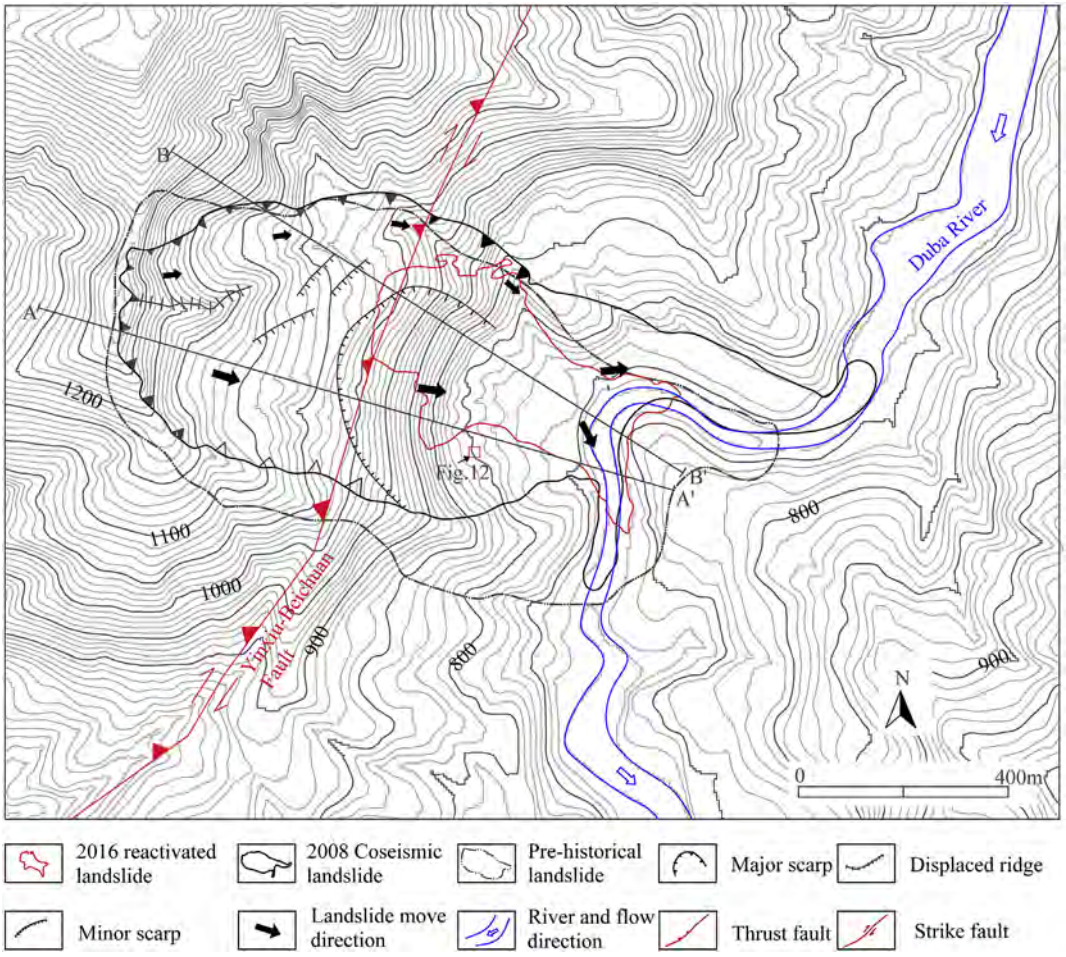

Fig. 7. Geomorphic map of the coseismic landslide occurred on May 12, 2008. The geological profiles along A-A′ and B-B′ are illustrated in Fig. 8.

based on before and after sliding DEM; open and export the attribute table of the cutfill result; summarize the depletion and accumulation volume respectively.

According to aforementioned procedure, total depletion volume and total accumulation volume are 3.91 million m^3 and 2.76 million m^3 for 2008 coseismic landslide, and 0.54 million m^3 and 0.69 million m^3 for 2016 reactivation landslide. Compared with previous study on a translational rock slide (Martha et al., 2010), the most distinguished characteristic of volume analysis on Tangjiawan landslides are two sets of volume loss and volume gain from the tail to toe of the landslides (see Fig. 14), confirming the suggestion about landslide mechanism in Section 3 that both 2008 and 2016 reactivation landslide in Tangjiawan site are composed of two sub-landslides. According to Fig. 14b, the volume loss of 2008 landslide majorly came from the west ridge of the slope where the ground surface elevation decreased 62.6 m at most, and from the gentle slope near the middle cliff. The highest accumulation depth appeared at the upstream part of the landslide dam, which also indicates the considerable erosion and remobilization in the downstream part of the landslide dam because the maximum ground elevation increase is supposed to appear at the downstream part of landslide on the same direction of main movement. Fig. 14c, d has higher resolution than Fig. 14a,b because of the better resolution and timely before- and after- sliding topographic map, and can show more details of volume variance along the whole landslide: 1) the major depletion and accumulation areas of 2016 landslide are along the main movement direction; 2) the upper depletion area of 2016 landslide with maximum depth of 32.5 m is located above the upstream part of the middle cliff, coinciding well with upper accumulation area of 2008 landslide; 3) the upper accumulation area of 2016 landslide lies near the toe of middle cliff, where is depletion area in 2008 event; 4) the lower depletion area of 2016 landslide is located in the flat terrace near the river channel where abundant deposits of 2008 landslide gathered.

The bulking factor (ratio of volume gain to volume loss) of 2008 coseismic landslide and 2016 reactivation landslide is 0.71 and 1.28 respectively. The abnormal bulking of 2008 event is due to two factors: 1) the 2011 DEM was used to calculate the 2008 landslide volume, therefore strong surface erosion and further remobilization during the three-year period after 2008, reducing the volume of the lower deposition (dam) area; 2) the failure surface is partly covered by deposits, means the overlapping of the source and deposition area (see the upper slope in Fig. 8a), which is the limitation of the cutfill method. Compared with the results reported by Martha et al. (2010), the bulking of 2016 Tangjiawan landslide is reasonable, considering the effect of possible overestimation of the gain volume due to poor sorting of rock and debris fragments.

4.2. The influence of rupture surface location

As mentioned in the Section 4.1, the exposure of rupture surface will influence the efficiency of the multi-temporal DEMs-based volume analysis. Take the 2008 coseismic Tangjiawan landslide for example (see Fig. 8), the landslide consisted of two sub-landslides and had two distinct rupture surfaces. According to the landslide classification (Hungr et al., 2014), the upper sub-landslide is a rock rotational slide (rock slump) developed in the anti-dip slope, while the lower sub-landslide is a debris slide which displaced the old landslide and colluvium deposition. According to Fig. 8, the upper sub-landslide is a deep-seated landslide with average depth of 75 m, while the rupture surface

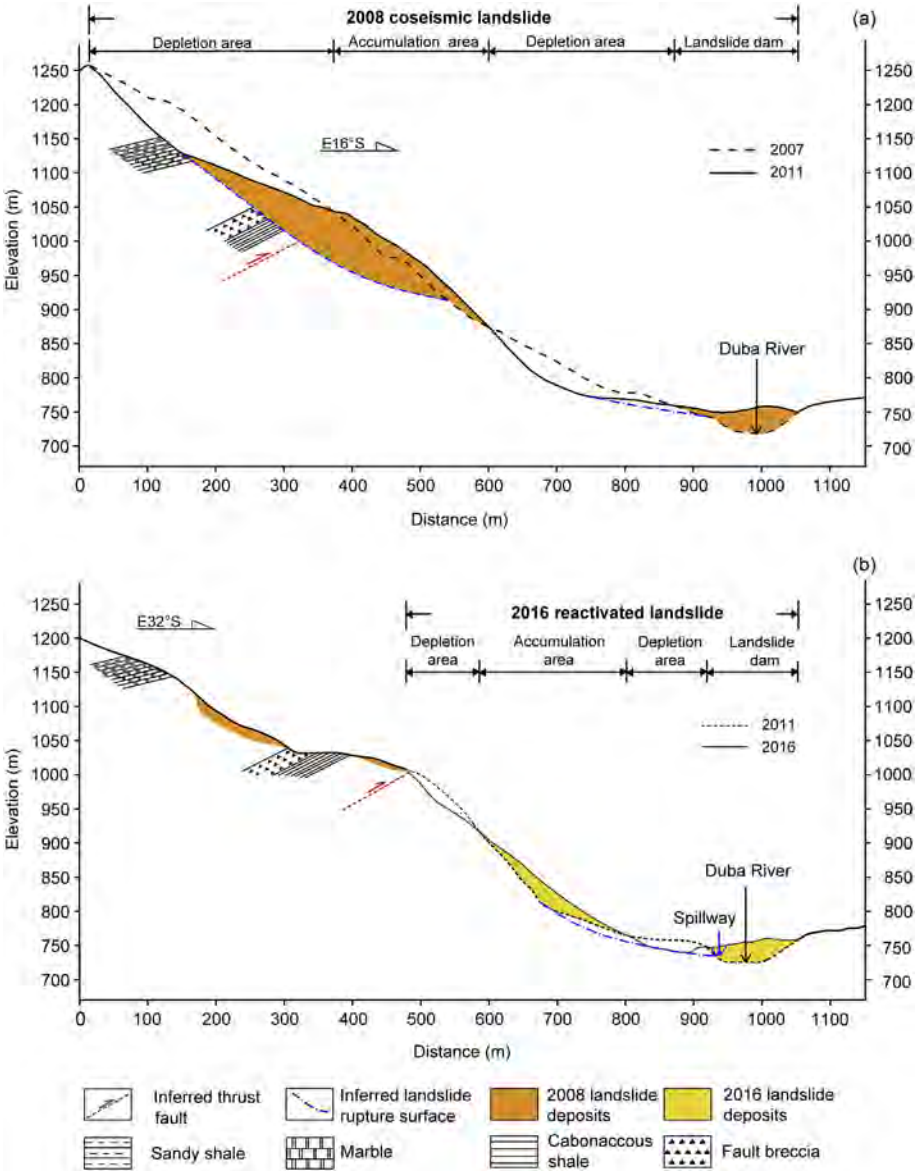

Fig. 8. Geological profiles of Tangjiawan landslides: (a) Profile of the 2008 coseismic landslide, corresponding to profile line A-A′ in Fig. 6; (b) profile of the 2016 reactivated landslide, corresponding to profile line B-B′ in Fig. 6. The fault plane was interpreted based on Dai et al., 2011.

of the lower sub-landslide is inferred to be about 15 m deep under the ground. Because of the rapid movement of the lower sub-landslide and namely a small overlap of the depletion and accumulation area, the volume of its source material and the landslide dam are 1.76 million m^3 and 1.553 million m^3, which show a small difference. However, the estimated depleted and accumulated volume of the upper sub-landslide is 2.064 and 1.096 million m^3 respectively, showing a significant difference. We inferred that huge difference was induced by the severe overlap of the source area and deposition area of the upper sub-landslide. If the unconsidered landslide volume was estimated through the area ratio with near depletion area on the slope profile (Fig. 8), the total depletion volume of 2008 coseismic landslide is 7.14 million m^3, which is 1.8 times than the result of the original cut-fill estimation, and 2.7 times than the estimation by Dai et al. (2011).

For the 2016 event, the volume analysis also indicates two depletion-accumulation sequences similar to the 2008 coseismic landslide. Combined the image analysis and the volume-analysis, the 2016 Tangjiawan reactivation landslide was suggested to consist of two sub-landslides with different mechanisms. The upper sub-landslide is a debris fall with irregular rupture surface and displaced the upper deposits of 2008 coseismic landslide of 0.29 million m^3 and 20 m deep on average. Since the rupture surface of upper sub-landslide is completed uncovered, it will not influence the volume estimation. The lower sub-landslide, consisting of deposits of 2008 landslide and older deposit and with average depth of 10 m, belongs to the debris slide which is inferred to be triggered by the drastic collision of upper debris fall. Considering the rupture surface of the lower sub-landslide is partially covered, its volume is reevaluated according to area ratio with second depletion area to 0.373 million m^3, which is 1.7 times than the original estimation.

Generally, the influence of rupture surface on the landslide volume estimation based on multi-temporal DEMs is decided by the landslide failure type and movement distance of the landslide. For rock/soil slides with short movement distance, the cutfill volume analysis will have relative large error, while it has considerable accuracy if the sliding mass displaced totally from the source area. This method is powerful in the estimating the volume of rock/debris fall, because this type of landslide has distinct source and deposition area. This method is also applicable in the rock/debris avalanche although it usually has three subareas including the source area, transition area and deposition

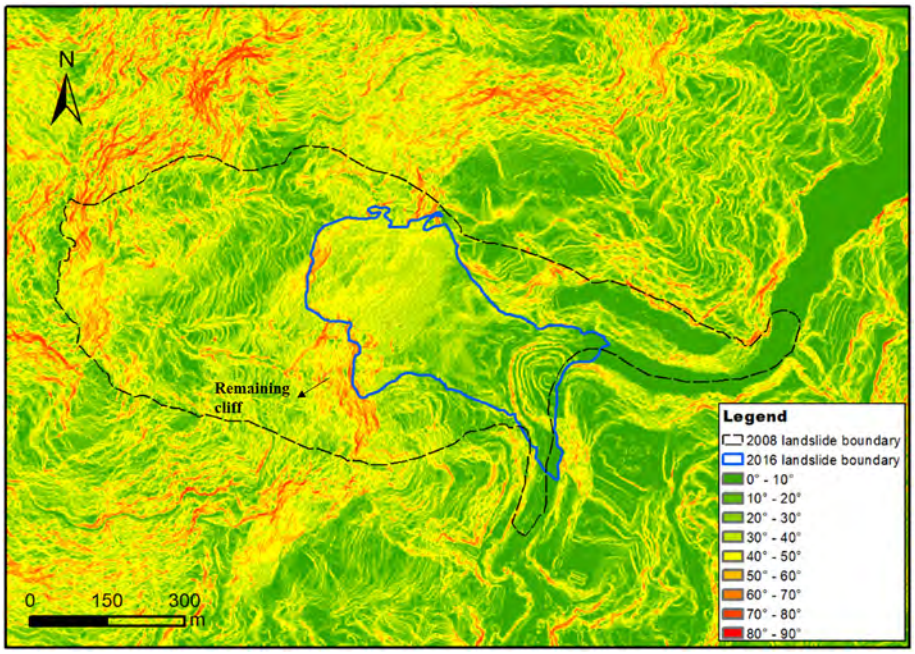

Fig. 9. Topographic gradient map of the Tangjiawan landslide based on the high-resolution DEM obtained by UAV survey in 2016.

area in which the latter two areas are usually partially overlapped.

4.3. Other limitations in volume estimation

With regard to the error of this multi-temporal DEMs-based volume analysis method, it is also affected by the resolution of different DEMs. The original resolution of 2008, 2011, 2016 DEM is 25 m, 5 m, 1 m respectively. While using the cutfill function to calculate the volumetric changes, the resolution of the output is decided by the relatively low resolution data. In other word, the spatial resolutions of volume measurement are 25 m for 2008 coseismic landslide and 5 m for 2016 landslide respectively (see Fig. 14). It is obvious that the accuracy of volume measurement through the multi-temporal DEMs will increase with higher-resolution DEMs. We used the resample function in ArcGIS to obtain resampled 2008, 2011, 2016 DEM with spatial resolution of 25 m, 5 m, and 1 m respectively, to which the same volume analysis procedure has been repeated accordingly. The results, including volume in the perspective of the whole landslide and major sections of landslide, acquired based on different DEM sequences are summarized in Table 1, which illustrates the influence of spatial resolution of

Fig. 10. The reactivation of the Tangjiawan landslide in September 2016, forming a landslide dam and barrier lake behind it: (a) the overview of the landslide; (b) the dam body; (c) the excavated spillway; and (d) the barrier lake.

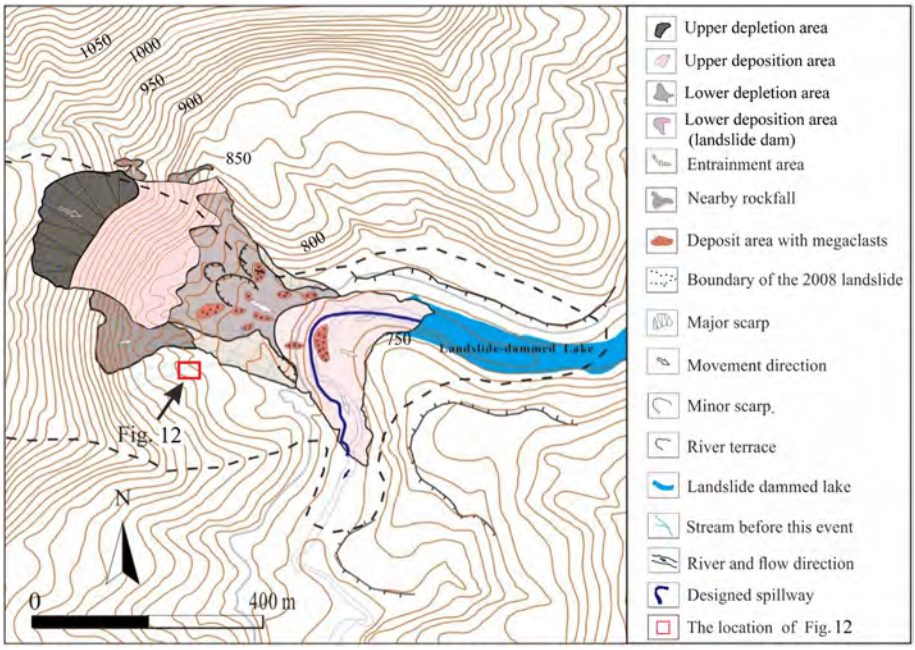

Fig. 11. Geomorphic map of the reactivated landslide occurred on September 6, 2016.

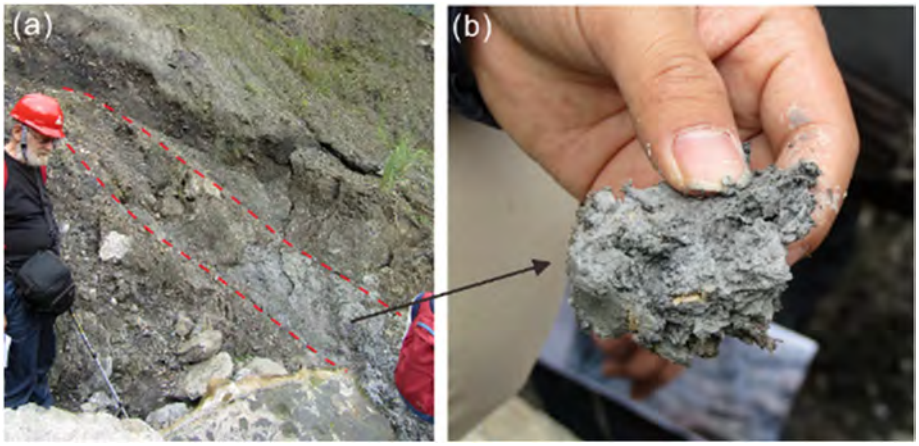

Fig. 12. (a) strongly disturbed and ruptured zone at the right (downstream) boundary of the landslide (the location is indicated in Fig. 11); (b) crushed plastic clay.

topographic map on the landslide volume estimation as the following: 1) with the spatial resolution of DEM enhanced, the bulking value of landslide volume estimation tends to be closer to 1.0, implying that careful check on the DEM data need to be completed before any physical description of the bulking value; 2) 5 m-resolution DEM will be precise enough for the volume estimation of such a magnitude of landslide (namely million m^3 size), since the relative error to volume estimated based on 1 m-resolution DEMs is no < 10% (estimated according to Table 1).

5. Hazard assessment and emergency response of the landslide dams

Landslide dams can result in considerable flooding hazard both in the upstream and/or in the downstream of the dam sites (Yang et al., 2013). Depend on the survival time and the risk level of the landslide dam, quick or detailed risk assessment of landslide dam is necessary before the implement of any hazard mitigation plan. Different empirical approaches were proposed to classify the risk level of a landslide dam

Table 1
Influence of the spatial resolution of topographic data on the landslide volume analysis.

Reactivation year	DEM resolution (m)	Volume loss (10^6m^3)	Volume gain (10^6m^3)	Bulking	Upper loss (10^6m^3)	Upper gain (10^6m^3)	Lower loss (10^6m^3)	Dam gain (10^6m^3)
2008	27	3.91	2.76	0.71	2.06	1.10	1.76	1.55
	5	3.57	3.12	0.87	1.88	1.59	1.60	1.30
	1	3.43	3.31	0.97	1.80	1.72	1.53	1.36
2016	27	0.54	0.74	1.37	0.46	0.31	0.26	0.24
	5	0.54	0.69	1.28	0.29	0.47	0.22	0.23
	1	0.58	0.65	1.12	0.32	0.42	0.23	0.23

Table 2
Summary of the key parameters of the landslide dams formed in 2008 and 2016.

Dam formation time	Dam width (m)	Dam length (m)	Dam height (m)	Dam volume (10^6 m^3)	Maximum capacity of lake (10^6 m^3)	Volume of lake before beaching (10^6 m^3)	Estimated overtopping time (days)	Composition material	Artificial breaching time	Designed spillway geometry (m)
May 12, 2008	850	154	38–42	3.12	6.88	1.56	31	Large blocks with diameter > 3 m (10%), boulders and fragments of 6–30 cm (60%), soil (30%)	June 6, 2008	length:413; width: 20; depth: 4
Sep 5, 2016	270	118	15–20	0.65	1.79	0.69	8	Boulders and fragments of 2–40 cm (28%); gravels and sands (58%); soil (14%)	Sep 6, 2016	length:260; width: 4; depth: 6

during the 2008 Wenchuan earthquake in China (Cui et al., 2009; Peng et al., 2014). A systematic approach for quick or detailed hazard evaluation of landslide dams contains four elements, namely, evaluation of dam-breach probability, assessment of upstream inundation hazard, assessment of downstream inundation hazard, and risk classification (Yang et al., 2013). The Tangjiawan landslide dammed the river twice, in 2008 and 2016, posing threats to > 2000 people downstream, provided uncommon examples to evaluate the performance of different quick or detailed landslide dam hazard assessment methods.

5.1. Stability evaluation of landslide dam

The dam geometry and volume of 2008 and 2016 Tangjiawan landslide were firstly obtained by image interpretation, DEM overlay, volume calculation and field measurements, see Table 2. We used the pre-earthquake DEM with a spatial resolution of 25-m to calculate the lake volume and coverage area for a given lake water level, and obtained the relation between the barrier lake volume and water level (Fig. 15). The inflow discharge rate is estimated as the ratio between the water volume increase ΔV and time difference ΔT for increasing the water level by certain value ΔH (Yang et al. (2013). A 28-h water level rising data gauged during 11 am on Sept 5th, to 15 pm on Sept 6th in 2016 indicated that the water level went up by 3.7 m during that period, suggesting that the average water inflow discharge is about 2.5 m^3/s. The relation between barrier lake volume and water level (Fig. 15) together with the lake inflow discharge can be employed to predict the dam overtopping time. Using this method, we calculated the time needed for the lakes to reach a certain level in Table 2. The results show that the dam formed in 2008 would have been overtopped on June 13, 2008 (31 days after the dam was formed), while the one formed in 2016 on September 14, 2016 (8 days after the dam was formed).

Rapid assessment of dam stability and hazard is a foremost step for landslide dam emergency response. A matrix was proposed after the Wenchuan earthquake for this purpose, using the height and constituent material of landslide dams as well as the maximum capacity of barrier lakes as three main criteria (Xu et al., 2009 and Cui et al., 2009). The landslide dam hazard is classified into four grades including very high, high, moderate and low (Table 3). Based on the parameters of the Tangjiawan dams in Table 2, the dam formed in 2008 is estimated to have high hazard, while the 2016 dam has moderate hazard, which is consistent with our field judgment.

Some studies also used morphometric factors, such as landslide dam volume and dimensional features (height, width and length), impounded-lake volume, upper catchment area, peak flow of the dammed stream etc. to predict landslide dam stability in a semi-quantitative way. For example, Ermini and Casagli (2003b) defined a new geomorphic dimensionless index (DBI, blockage index) by combining dam height (H_d, m), volume (V_d, m^3) and upper catchment area (A_b, m^2).

$$DBI = \log\left(\frac{A_b \times H_d}{V_d}\right) \quad (1)$$

If DBI < 2.75, the dam is considered stable; if DBI varies from 2.75 to 3.08, the dam stability is uncertain; and if DBI > 3.08, the dam is unstable. Using the geomorphic variables in Table 2, the DBI of the dams formed in 2008 and 2016 is calculated to be 2.83 (uncertain) and 3.21 (unstable), respectively (A_b is measured as 60×10^6 m^2).

A new geomorphological index (HDSI, hydromorphological dam stability index) is defined by Stefanelli et al. (2016) for landslide dam stability evaluation, which can consider the erosive capacity of the stream S besides with landslide volume V and upstream catchment area A_b.

$$HDSI = \log\left(\frac{V}{A_b \times S}\right) \quad (2)$$

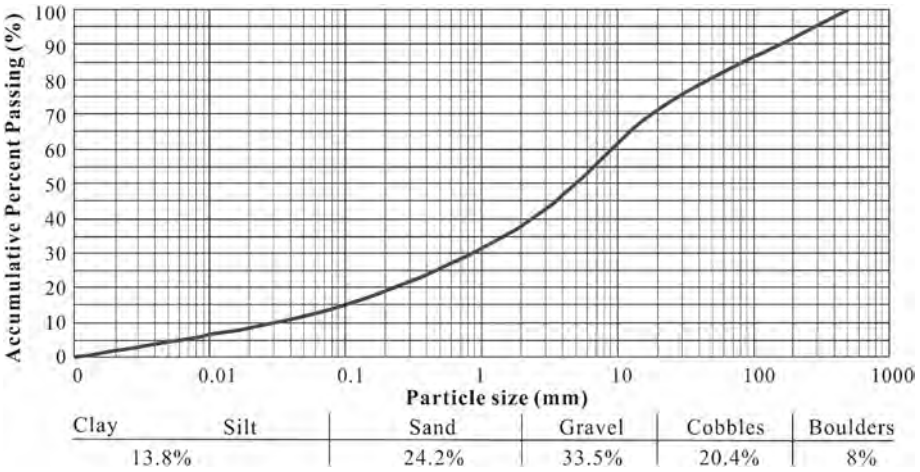

Fig. 13. The accumulative grain-size distribution curve obtained using the terrestrial laser scanning (TLS) data.

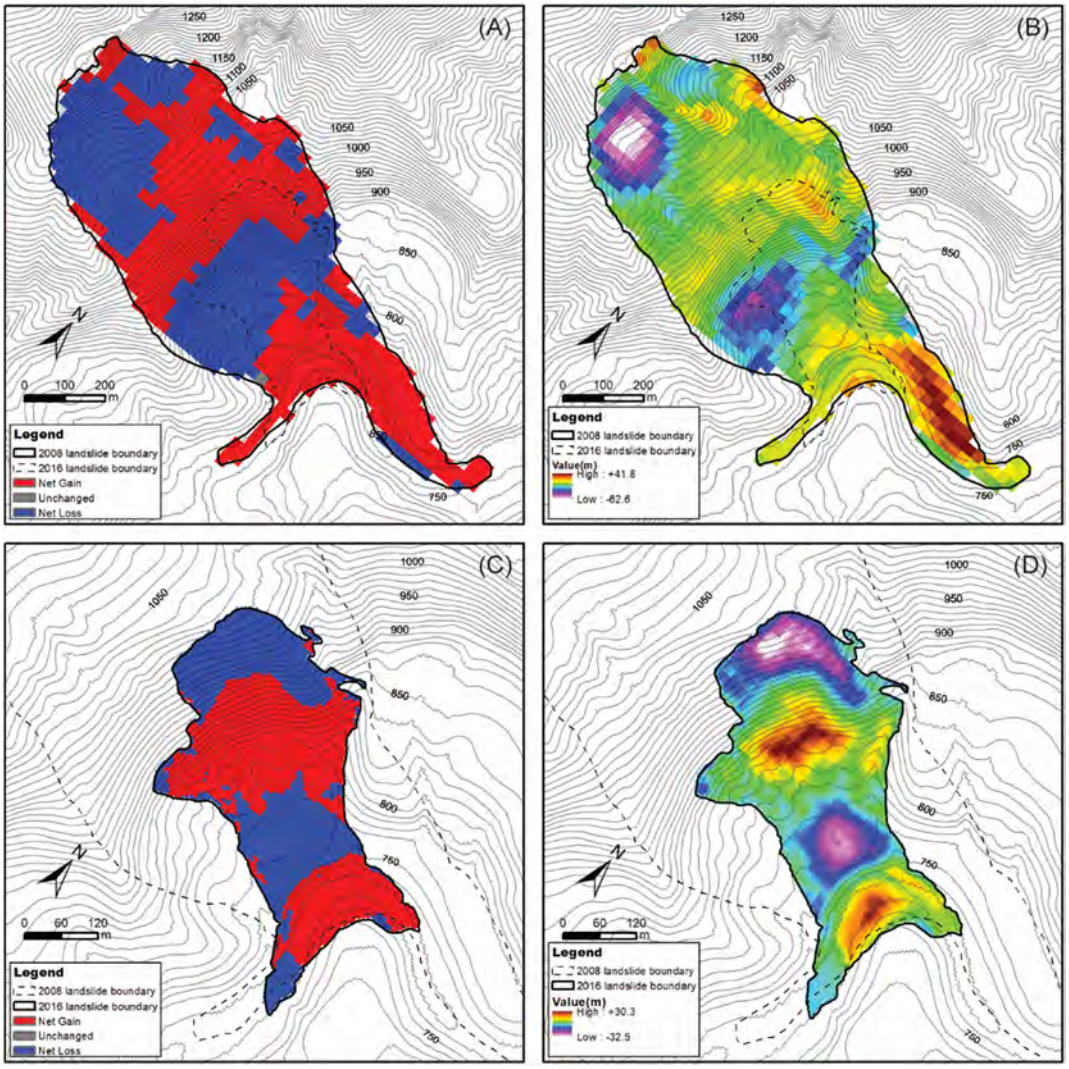

Fig. 14. Volume analysis of the 2008 coseismic and 2016 reactivation landslide in the Tangjiawan site: (A), (C) Extent of the volume loss and volume gain, which corresponds to the zones of depletion and accumulation for the 2008 landslide and 2016 landslide, respectively. (B), (D) Elevation difference due to 2008 landslide and 2016 landslide respectively, with negative values showing the lowering of surface and positive values showing the rising of the surface after the event. (A) and (B) have spatial resolution of 25 m, while (C) and (D) have spatial resolution of 5 m.

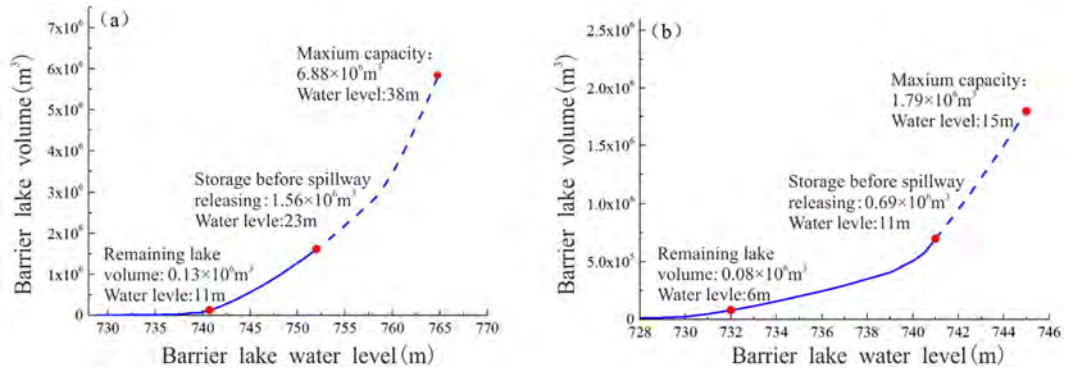

Fig. 15. Relationship between the volume and the water level of the barrier lakes formed in 2008 (a) and 2016 (b).

Table 3
Matrix for a quick assessment of the individual landslide dams induced by the Wenchuan earthquake.

Hazard category	Criteria		
	Dam height (m)	Maximum capacity of barrier lake ($10^4 m^3$)	Composing materials of dam
Very high	> 100	> 10^4	Soil texture dominated
High	50–100	10^3–10^4	Soil texture with some big rocks
Moderate	25–50	10^2–10^3	Big rocks with soil
Low	< 25	< 10^2	Big rocks dominated

where V is the landslide volume (m^3), A_b is the catchment area upstream of the blockage point (km^2), S is local slope of the channel bed (m/m) that indicate the hydrological erosive capacity.

If HDSI > 7.44, the dam is considered stable; if HDSI varies from 5.74 to 7.44, the dam stability is uncertain; and if HDSI < 5.74, the dam is unstable. Using the geomorphologic parameters in Table 2, the HDSI of the dams formed in 2008 and 2016 is evaluated to be 6.55 (uncertain) and 5.87 (uncertain, but very close to unstable).

Dong et al. screened out the main geomorphic parameters that influence the stability of landslide dams and established discriminant models and logistic regression models with four major geomorphic parameters for rapidly evaluating the landslide dam stability and failure probability (Dong et al., 2009, 2011a, b). The model inputs include peak discharge P flowing into the barrier lake, upstream catchment area A_b, and the common geometric parameters of the landslide dam, such as the height H, the length L, and the width W of the dam. The discriminant models indicated as PHWL_Dis and AHWL_Dis, and the logistic regression models indicated as PHWL_Log and AHWL_Log, are illustrated in the Eq. (3) to (7), respectively. When the peak flow charge P is not available during the landslide dam stability rapid assessment, the upstream catchment area A_b can replace peak flow charge P as the model inputs. In other words, when P is unknown, the AHWL_Dis and AHWL_Log models are suggested.

$$D_s = -2.94\log(P) - 4.58\log(H_d) + 4.17\log(W_d) + 2.39\log(L_d) - 2.52 \quad (3)$$

$$D_s = -2.62\log(A_b) - 4.67\log(H_d) + 4.57\log(W_d) + 2.67\log(L_d) + 8.26 \quad (4)$$

$$L_s = -2.55\log(P) - 3.64\log(H_d) + 2.99\log(W_d) + 2.73\log(L_d) - 3.87 \quad (5)$$

$$L_s = -2.22\log(A_b) - 3.76\log(H_d) + 3.17\log(W_d) + 2.85\log(L_d) + 5.93 \quad (6)$$

where D_s is the discriminant score (dimensionless); L_s is the logit score (dimensionless); P is peak inflow discharge (m^3/s); A_b is the catchment area upstream of the blockage point (m^2); H_d is dam height (m); W_d is dam width (m); L_d is dam length (m).

A landslide dam with $D_s > 0$ or Ls > 0 is classified into stable group, and that with $D_s < 0$ or Ls < 0 is classified into unstable group. Using the geomorphologic parameters in Table 2, the D_s of the dams formed in 2008 and 2016 are evaluated to be −0.47 (unstable) and −1.55 (unstable), and L_s of the them are evaluated to be −1.92 and −2.62. Moreover, the failure probability of a landslide dam can be related to the logit Ls using the following equation (Menard 2002; Yang et al., 2013).

$$P_f = \frac{e^{-L_s}}{1 + e^{-L_s}} \quad (7)$$

Based on the above equation, the failure probability (P_f) of the dams formed in 2008 and 2016 are 87% and 93%, corresponding to high and extremely high level of dam failure probability, respectively (Yang et al., 2013).

Therefore, according to the above qualitative and semi-quantitative

Table 4
Comparison of predictions of dam stability of the two Tangjiawan landslide dams from different empirical equations.

Empirical equations	Reference	Stability index[a]	
		2008 event	2016 event
$DBI = \log\left(\frac{A_b \times H_d}{V_d}\right)$	Ermini and Casagli, 2003a, b	2.83(UC)	3.21(US)
$HDSI = \log\left(\frac{V}{A_b \times S}\right)$	Stefanelli et al., 2016	6.55(UC)	5.87(UC)
$D_s = -2.94\log(P) - 4.58\log(H_d) + 4.17\log(W_d) + 2.39\log(L_d) - 2.52$	Dong et al., 2009	−0.66(US)	−1.54(US)
$D_s = -2.62\log(A_b) - 4.67\log(H_d) + 4.57\log(W_d) + 2.67\log(L_d) + 8.26$	Dong et al., 2009	−0.47(US)	−1.55(US)
$L_s = -2.55\log(P) - 3.64\log(H_d) + 2.99\log(W_d) + 2.73\log(L_d) - 3.87$	Dong et al., 2011a, b	−2.12(US)	−2.75(US)
$L_s = -2.22\log(A_b) - 3.76\log(H_d) + 3.17\log(W_d) + 2.85\log(L_d) + 5.93$	Dong et al., 2011a, b	−1.92(US)	−2.62(US)

Note: UC means uncertain stability; US means unstable.
[a] The letter in the brackets behind each stability index indicates the stability evaluation results corresponding to each empirical model.

Table 5
Comparison of predictions of the peak discharge of the two Tangjiawan landslide dam from different empirical equations.

Empirical equations	Reference	Peak discharge Q_p, (m^3/s)	
		2008 event	2016 event
$Q_p = 6.3H_d^{1.59}$	Costa, 1985	2401	738
$Q_p = 0.72V_l^{0.53}$	Evans, 1986	1379	895
$Q_p = 672V_l^{0.56}$	Costa and Schuster, 1988	862	546
$Q_p = 6.7d^{1.73}$	Walder and O'Connor, 1997	1408	360
$Q_p = 1.60V_0^{0.46}$	Walder and O'Connor, 1997	1130	776
$Q_p = 181(H_dV_l)^{0.43}$	Costa and Schuster, 1988	1093	560
$Q_p = 0.99(dV_0)^{0.40}$	Walder and O'Connor, 1997	1023	538
$Q_p = 0.0158(PE)^{0.41}$	Costa and Schuster, 1988	856	453
$Q_p = 0.063(PE)^{0.42}$	Clague and Evans, 2000	4453	2319
$\frac{Q_p}{g^{1/2}h_d^{5/2}} = \left(\frac{H_d}{h_r}\right)^{-1.371}\left(\frac{V_l^{1/3}}{H_d}\right)^{1.536} e^a$	Peng and Zhang, 2012	3524	3139
$Q_P = \frac{8}{27}\sqrt{g}\left(\frac{B}{b}\right)^{\frac{1}{4}} bH_o^{\frac{3}{2}}$	Li, 2006	3409	954

rapid assessment methods (summarized in Table 4), the stability of 2008 Tangjiawan landslide dam is evaluated as unstable except the results of DBI and HDSI which indicate uncertain stability, and that of 2016 landslide dam is evaluated as unstable except for result of HDSI method which is uncertain but very close to unstable.

5.2. Peak flow estimation of dam breach

In the emergency phase, empirical models are more convenient to be applied for estimating the potential dam-break flood parameters, as it does not require complicated geotechnical parameters of dam composition material and detailed topographic data as the physically based and numerical models do. Thus, we use empirical equations (Eqs. (8) to (10)) to present the key hydraulic impacts of flood on the downstream areas, including the peak discharge at dam site and different locations downstream as well as the flood arrival time (Li, 2006). The results are summarized in Table 5 and Table 6. The method has also been applied in previous studies (i.e. Liu et al., 2009; Cui et al., 2010; Fan et al., 2012b) to predict the peak discharge of the coseismic Tangjiashan landslide dam.

$$Q_{PL} = \frac{W}{\frac{W}{Q_P} + \frac{L}{VK}} \tag{8}$$

Table 6
Predicted dam-break flood parameters on the dam site and downstream area.

Locations	Distance from dam (km)	Prediction of flood of dam-break in 2008		Prediction of flood of dam-break in 2016	
		Peak discharge (m^3/s)	Peak arrival time (min)	Peak discharge (m^3/s)	Peak arrival time (min)
Dam site	0	3409	0.0	954	0.0
Taihong bridge	0.2	3213	0.2	918	0.3
Cuijiayuanzi	0.5	2957	0.6	870	1.1
Jinggu bridge	5	1348	14.1	485	28.5
Chengjiaba	9.5	873	34.7	336	69.9

where L is the distance from the dam (m); W is the barrier lake volume before breaching (m^3); Q_P is the peak discharge at the dam (m^3/s), and VK is an empirical coefficient, equaling to 3.13 for rivers on plains, 7.15 for mountain rivers, and 4.76 for rivers flowing through the terrain with intermediate relief (Li, 2006). The peak discharge, Q_P at the dam (m^3/s), could be calculated by Eq. (9):

$$Q_P = \frac{8}{27}\sqrt{g}\left(\frac{B}{b}\right)^{\frac{1}{4}} bH_o^{\frac{3}{2}} \tag{9}$$

where B is the width of the dam crest (m), H_0 is the lake water level before dam failure (m), g is the acceleration of gravity (9.8 m/s^2), and b is the width of the breach (m).

According to the flood travel time equation (Li, 2006) developed by the Institute of Hydraulic Research of the Yellow River Conservancy Commission on physical model experiments, the peak arrival time (t in the unit of second) downstream from a landslide dam could be calculated by Eq. (10).

$$t = k\frac{L^{1.4}}{W^{0.2}H_0^{0.5}h_m^{0.25}} \tag{10}$$

where k is a coefficient, varying from 0.8 to 1.2, h_m is the water depth at maximum discharge after dam failure, could be calculated by $H_o/10^{0.3b/B}$.

The predicted peak discharge (Q_p) calculated through Eq. (9) are 3409 and 953 m^3/s for 2008 co-seismic and 2016 reactivation landslide dam at the Tangjiawan site, respectively. Both the lake volume and water level height before breaching for 2008 landslide are more than two times larger than the ones for 2016 landslide, and the peak discharge of 2008 landslide predicted using Eq. (9) is about 3.6 times larger than that of 2016 landslide. We suggest these predictions are relatively reasonable because the importance of lake volume and water level height before breaching is significant in almost all published models. Another reason supporting the adaptability of Eq. (9) is that it brings in the breach width as an important input, which is consistent with the fact that many landslide dams in Wenchuan earthquake area are breached manually using the spillway with certain design breach width.

We compared the results predicted through Eq. (9) with the ones estimated by other different empirical models in Table 5. These models are based on single or combined parameters of landslide dam including the barrier lake volume (V_l), dam height (H_d), dam width (W_d), breach width (b), dam volume (V_d), dam length(B), drop in water level (d), released water volume (V_o), and the potential energy (PE), which is the product of dam height, lake volume, and specific weight of water. The predicted peak discharge Q_p of these empirical models varies from 856 to 4453 m^3/s, with an average of 2111 m^3/s for the 2008 co-seismic Tangjiawan landslide dam, while it varies from 360 to 3319 m^3/s, with an average of 1181 m^3/s for the 2016 event. The deviations of different empirical models might result from site-specific characteristics of the original sample landslide dams in different study areas.

The one-variable equations tend to underestimate the peak discharge compared to the results of the Eq. (9). The two-variable equations considering the lake volume or water release volume, and dam height or water level drop height have similar prediction. The peak discharge prediction varies significantly for potential energy models build by different researchers. In the Tangjiawan case, the equation proposed by Peng and Zhang (2012) provides the closest prediction compared to the results of the Eq. (9) for 2008 landslide event, while limited prediction difference for 2008 and 2016 event. We find that the equation proposed by Peng and Zhang (2012) is sensitive to the parameter "a" which equates 1.236 for high erodibility dams, −0.380 for medium erodibility dams, and − 1.615 for low erodibility dams, compared to other input parameters. For example, the peak discharge estimated through Peng (2012) model under the condition of high erodibility can be five times larger than the results under the medium

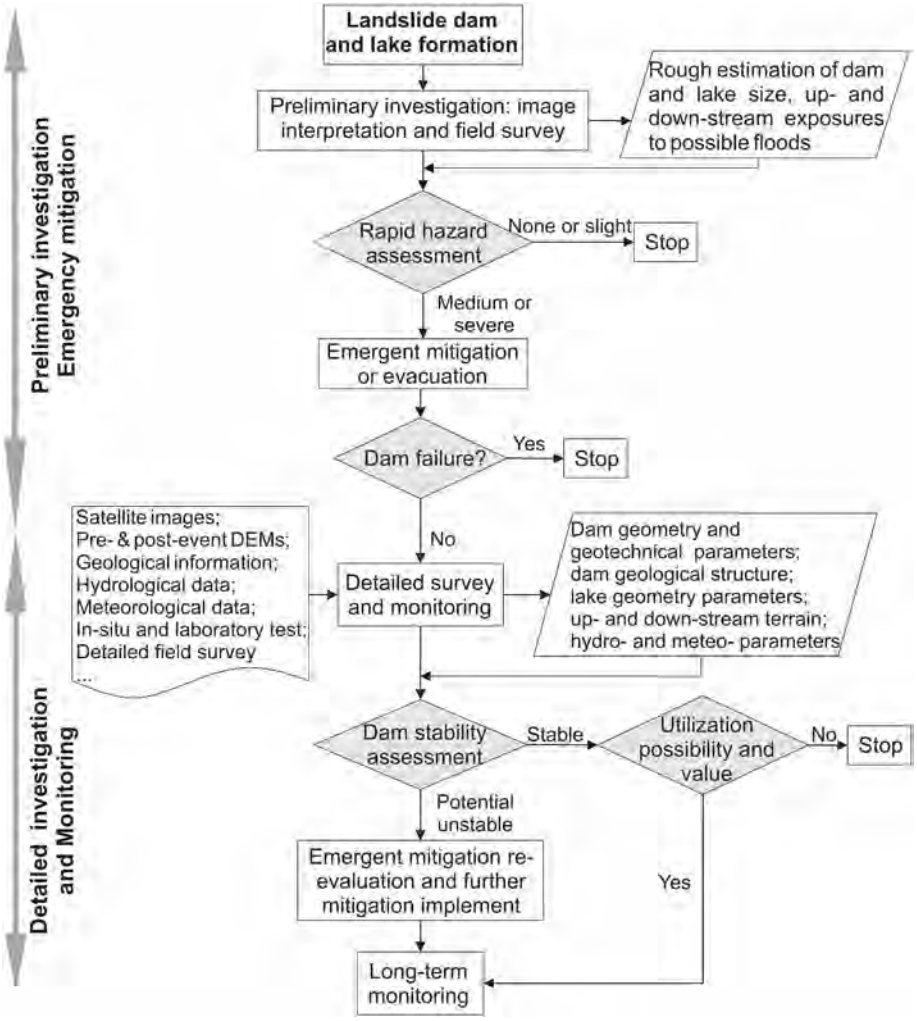

Fig. 16. A generalized work procedure after a landslide dam is formed.

erodibility assumption for both the 2008 and 2016 Tangjiawan landslide dam.

It can be seen from Table 6 that the peak discharge of the potential dam-break flood in 2008 is nearly four times higher than that in 2016, due to the larger impounded lake in 2008. The 10 years return period flood measured by the nearby hydrological station is about 883 m^3/s. Therefore, if the dam breached naturally in 2008, the biggest town downstream, the Chengjiaba would have experienced a flood with an equivalent of nearly 10 year return period (873 m^3/s) within 40 min after the dam beaching, see Table 6. The potential dam-beach flood in 2016 is estimated to have a peak discharge of 336 m^3/s, and the peak will arrive about one hour after the dam failure. Using the flooding hazard index I_{db} defined by Yang et al. (2013) as the ratio of predicted peak outburst flow discharge and the allowable discharge for certain river section (here assumed as 611 m^3/s, equivalent to a flood with 5 year return period). The I_{db} of the 2008 and 2016 landslide dam are 1.43 and 0.55, corresponding to extremely high and middle flooding hazard, respectively (Yang et al., 2013).

5.3. Hazard assessment and emergency response

Using the landslide dam flooding risk matrix developed by Yang et al. (2013) combined the dam-failure probability and flooding hazard (evaluated in Sections 5.1 and 5.2), the flooding risk of 2008 and 2016 landslide dam are classified as extremely high and high, respectively. Due to the high potential risk of the 2008 and 2016 damming events, artificial control measures were carried out by constructing a spillway across the landslide dam to reduce the water level and volume of the dammed lakes. The geometry of the spillways is shown in Table 2. The path of the spillway crossing landslide dam should be determined with the consideration of the lowest point of the dam crest, the dam composition materials, the dam geometry features and the original river course. In any case, spillway excavation should avoid the disturbance of main landslide deposits and should normally start from the downstream of dams. The cross section of spillways is often trapezoidal to avoid the side collapse, especially for the deep ones. The spillway gradient should normally be controlled under 1% in order to reduce the flow speed and erosion. Comparing Fig. 3 (a) with (b), it can be seen that the spillway constructed in 2008 follows the original river course, so does the one in 2016. The spillway gradient in both case varies from 5‰ to 7‰, and the side slope of 1:1.5 to 1:2.0.

Based on the experience and the lessons learned from the emergency mitigation of landslide dams induced by the Wenchuan earthquake, we propose a general work procedure for landslide dam mitigation after a lake is identified (Fig. 16). This procedure can be generally divided into two phases: rapid assessment of damming hazard and emergency mitigation based on preliminary investigation of landslide dams (which normally should be done within two weeks); and detailed investigation and monitoring of the relatively large dams that may be temporarily stabilized by emergency mitigation measures but still have a considerable failure probability. Estimation of the geometry and geomorphic parameters of landslide dams and barrier lakes as well as

potential up- and down-stream exposures is crucial for the rapid risk assessment. Remote sensing is a very effective tool to this goal, which is more and more commonly used especially with the development of UAV. In this study we used UAV to obtain the high-resolution image and DSM to calculate the dam volume and to make detailed geomorphic mapping together with field investigation. Detailed investigation could only be done if a dam is evaluated to be temporally stable. In-situ and laboratory tests could be implemented to obtain the geotechnical parameters and dam geological structure features in order to make a more reliable assessment of dam stability. In a few cases, landslide dams could be utilized for hydropower generation (i.e. Zhang et al., 2015).

6. Conclusions

The paper presents the successive landslide dam formation by different landslide triggering and failure mechanism taken the Tangjiawan landslide in the Wenchuan earthquake hit region as an example. The landslide is considered as an old landslide that occurred probably many years before the earthquake, according to supportive evidences from field investigation and image interpretation. It was reactivated by the 2008 Wenchuan earthquake as the main fault (Yingxiu-Beichuan fault) passing through the upper part of the slope. The thrusting of the fault initiated the landslide, which is consistent with the conclusion of previous studies (i.e. Dai et al., 2011). Part of the coseismic landslide was reactivated again in Sep 2016, and blocked the Duba River at the same location as the dam formed by the coseismic landslide. There was no direct triggers of the new reactivation, which was inferred as the combination effect of high tectonic uplift rate, the decease of yield strength due to seismic shaking, antecedent rainfall and erosion of the slope foot by the river over many years. Multi-temporal DEMs are used to conduct the volume analysis of the two landslides, whose results contribute to the landslide mechanism analysis and suggest that the landslide type, landslide rupture surface, as well as the resolution of DEM, influence the landslide volume estimation significantly. Generally, the successive landslide dams at the Tangjiawan site are caused by the successive landslide reactivations on an anti-dip slope evolving under the effects of strong tectonic activity and river erosion, and remobilizing a mass of loose materials of previous landslide deposition. Considering the remain landslide deposition on the upper slope, this site is still possible to encounter landslide dam hazard in the future. In spite of the different triggering mechanism, the 2008 and 2016 Tangjiawan landslide dam indicate an extremely high and high level of flooding risk for downstream areas through the quick assessment of dam stability and outburst flood parameters based on different empirical models. Spillways were used as an emergency engineering measure to mitigate the potential hazard of the two landslide dams.

Acknowledgement

This research is financially supported by National Science Fund for Outstanding Young Scholars of China (Grant No. 41622206), the Funds for Creative Research Groups of China (Grant No. 41521002), the Fund for International Cooperation (NSFC-RCUK_NERC, Grant No. 4151101239), Resilience to Earthquake-induced landslide risk in China (Grant No. 41661134010), the Fok Ying-Tong Education Foundation for Young Teachers in the Higher Education Institutions of China (Grant No. 151018) and the AXA fund. The authors thank Dr. Mauri McSaveney for his support in field investigation.

References

Adams, J., 1981. Earthquake-dammed lakes in New Zealand. Geology 9 (5), 215–219.
Cenderelli, D.A., 2000. Floods from natural and artificial dam failures. In: Wohl, E.E. (Ed.), Inland Flood Hazards. Cambridge University Press, New York, pp. 73–103.
Chen, R.F., Chang, K.J., Angelier, J., Chan, Y.C., Deffontaines, B., Lee, C.T., Lin, M.L., 2006. Topographical changes revealed by high-resolution airborne LiDAR data: the 1999 Tsaoling landslide induced by the Chi–Chi earthquake. Eng. Geol. 88 (3), 160–172.
Chen, X., Cui, P., You, Y., Chen, J., Li, D., 2015. Engineering measures for debris flow hazard mitigation in the Wenchuan earthquake area. Eng. Geol. 194, 73–85.
Clague, J.J., Evans, S.G., 2000. A review of catastrophic drainage of moraine-dammed lakes in British Columbia. Quat. Sci. Rev. 19, 1763–1783.
Costa, J.E., 1985. Floods from dam failures (no. 85–560). In: US Geological Survey.
Costa, J.E., Schuster, R.L., 1988. The formation and failure of natural dams. Geol. Soc. Am. Bull. 100, 1054–1068.
Cui, P., Zhu, Y.Y., Han, Y.S., Chen, X.Q., Zhuang, J.Q., 2009. The 12 May Wenchuan earthquake-induced landslide lakes: distribution and preliminary risk evaluation. Landslides 6 (3), 209–223.
Cui, P., Dang, C., Zhuang, J., You, Y., Chen, X., Scott, K.M., 2010. Landslide-dammed lake at Tangjiashan, Sichuan Province, China (triggered by the Wenchuan earthquake, May 12, 2008): risk assessment, mitigation strategy, and lessons learned. Environ. Earth Sci. http://dx.doi.org/10.1007/s12665-010-0749-2.
Dai, F.C., Lee, C.F., Deng, J.H., Tham, L.G., 2005. The 1786 earthquake-triggered landslide dam and subsequent dam-break flood on the Dadu River, southwestern China. Geomorphology 65 (3–4), 205–221.
Dai, F.C., Tu, X.B., Xu, C., Gong, Q.M., Yao, X., 2011. Rock avalanches triggered by oblique-thrusting during the 12 may 2008 Ms 8.0. Geomorphology 132, 300–318.
Dong, J.J., Tung, Y.H., Chen, C.C., Liao, J.J., Pan, Y.W., 2009. Discriminant analysis of the geomorphic characteristics and stability of landslide dams. Geomorphology 110 (3–4), 162–171.
Dong YH, Luo SM, Han YP, Chen CY. (2011a). Co-and post-seismic vertical displacements of Wenchuan Ms8. 0 earthquake near Beichuan. Geodesy and Geodynamics, 2(2), 29–32.
Dong, J.J., Tung, Y.H., Chen, C.C., Liao, J.J., Pan, Y.W., 2011b. Logistic regression model for predicting the failure probability of a landslide dam. Eng. Geol. 117 (1–2), 52–61.
Ermini, L., Casagli, N., 2003a. Prediction of the behaviour of landslide dams using a geomorphological dimensionless index. Earth Surf. Process. Landforms 28 (1), 31–47.
Ermini, L., Casagli, N., 2003b. Prediction of the behaviour of landslide dams using a geomorphological dimensionless index. Earth Surf. Process. Landf. 28 (1), 31–47.
Evans, S.G., 1986. The maximum discharge of outburst floods caused by the breaching of man-made and natural dams. Can. Geotech. J. 23 (3), 385–387.
Evans, S., Delaney, K., Hermanns, R., Strom, A., Scarascia-Mugnozza, G., 2011. The formation and behaviour of natural and artificial rockslide dams; implications for engineering performance and hazard management. In: Evans, S.G., Hermanns, R.L., Strom, A., Scarascia-Mugnozza, G. (Eds.), Natural and Artificial Rockslide Dams. 133. Springer Berlin Heidelberg, pp. 1–75.
Fan, X.M., van Westen, C.J., Xu, Q., Görüm, T., Dai, F., 2012a. Analysis of landslide dams induced by the 2008 Wenchuan earthquake. J. Asian Earth Sci. 57, 25–37.
Fan, X.M., Tang, C.X., van Westen, C.J., Alkema, D., 2012b. Simulating dam-breach scenarios of the Tangjiashan landslide dam induced by the Wenchuan earthquake. Nat. Hazards Earth Syst. Sci. 12, 3031–3044.
Görüm, T., Fan, X.M., van Westen, C.J., Huang, R.Q., Xu, Q., Tang, C.X., Wang, G., 2011. Distribution pattern of earthquake-induced landslides triggered by the 12 May 2008 Wenchuan earthquake. Geomorphology 133 (3–4), 152–167.
Hungr, O., Leroueil, S., Picarelli, L., 2014. The Varnes classification of landslide types, an update. Landslides 11 (2), 167–194.
Korup, O., 2004. Geomorphometric characteristics of New Zealand landslide dams. Eng. Geol. 73 (1–2), 13–35.
Korup, O., Tweed, F., 2007. Ice, moraine, and landslide dams in mountainous terrain. Quat. Sci. Rev. 26 (25), 3406–3422.
Li, W., 2006. Handbook of Hydraulic Calculations. Water Publication, Beijing (in Chinese).
Li, X., Zhou, Z., Yu, H., Wen, R., Lu, D., Huang, M., Zhou, Y., Cu, J., 2008. Strong motion observations and recordings from the great Wenchuan Earthquake. Earthq. Eng. Eng. Vib. 7 (3), 235–246.
Liu, N., Zhangj, Lin W., Cheng, W., Chen, Z., 2009. Draining Tangjiashan Barrier Lake after Wenchuan Earthquake and the flood propagation after the dam break. Sci. China E 52 (4), 801–809.
Martha, T.R., Kerle, N., Jetten, V., van Westen, C.J., Kumar, K.V., 2010. Landslide volumetric analysis using Cartosat-1-derived DEMs. IEEE Geosci. Remote Sens. Lett. 7 (3), 582–586.
Mason, K., 1929. Indus floods and Shyok glaciers. Himalayan J. 1, 10–29.
Menard, S., 2002. Applied logistic regression analysis, 2nd edn. Sage, Thousand Oaks.
Peng, M., Zhang, L.M., 2012. Breaching parameters of landslide dams. Landslides 9 (1), 13–31.
Peng, M., Zhang, L.M., Chang, D.S., Shi, Z.M., 2014. Engineering risk mitigation measures for the landslide dams induced by the 2008 Wenchuan earthquake. Eng. Geol. 180, 68–84.
Shang, Y., Yang, Z., Li, L., Liu, D.A., Liao, Q., Wang, Y., 2003. A super-large landslide in Tibet in 2000: background, occurrence, disaster, and origin. Geomorphology 54 (3), 225–243.
Shen, Z.K., Sun, J., Zhang, P., Wan, Y., Wang, M., Bürgmann, R., ... Wang, Q., 2009. Slip maxima at fault junctions and rupturing of barriers during the 2008 Wenchuan earthquake. Nat. Geosci. 2 (10), 718.
Shi, Z.M., Wang, Y.Q., Peng, M., Chen, J.F., Yuan, J., 2015. Characteristics of the landslide dams induced by the 2008 Wenchuan earthquake and dynamic behavior analysis using large-scale shaking table tests. Eng. Geol. 194, 25–37.
Stefanelli, C.T., Catani, F., Casagli, N., 2015. Geomorphological investigations on landslide dams. Geoenviron. Disasters 2 (1), 21.
Stefanelli, C.T., Segoni, S., Casagli, N., Catani, F., 2016. Geomorphic indexing of landslide dams evolution. Eng. Geol. 208, 1–10.

Walder, J.S., O'Connor, J.E., 1997. Methods for predicting peak discharge of floods caused by failure of natural and constructed earthen dams. Water Resour. Res. 33 (10), 2337–2348.
Xu, Q., Fan, X.M., Huang, R.Q., Westen, C., 2009. Landslide dams triggered by the Wenchuan Earthquake, Sichuan Province, south west China. Bull. Eng. Geol. Environ. 68 (3), 373–386.
Yang, S.H., Pan, Y.W., Dong, J.J., Yeh, K.C., Liao, J.J., 2013. A systematic approach for the assessment of flooding hazard and risk associated with a landslide dam. Nat. Hazards 65 (1), 41–62.
Zhang, S.J., Xie, X.P., Wei, P.Q., Chernomorets, S., Petrakov, D., Pavlova, I., Tellez, R.D., 2015. A seismically triggered landslide dam in Honshiyan, Yunnan, China: from emergency management to hydropower potential. Landslides 12, 1147–1157.